Available online at www.sciencedirect.com
ScienceDirect
Environmental Modelling & Software 22 (2007) 823–836
Environmental Modelling & Software
www.elsevier.com/locate/envsoft

AFFDEF: A spatially distributed grid based rainfall–runoff model for continuous time simulations of river discharge

Greta Moretti [a,*], Alberto Montanari [b]

[a] Ingenieurbüro Winkler und Partner GmbH, Schlossstrasse 59a, 70176 Stuttgart, Germany
[b] Faculty of Engineering, University of Bologna, Via del Risorgimento 2, I-40136 Bologna, Italy

Received 1 September 2004; received in revised form 22 November 2005; accepted 28 February 2006
Available online 23 August 2006

Abstract

This paper aims to present a rainfall-runoff model that was recently released into the public domain via the World Wide Web. The model, AFFDEF, is spatially distributed (grid based) and performs continuous time simulations of river flows at any time step and at any location in the catchment. It does not, however, account for snowmelt. Conceptual and physically based schemes are employed for simulating the rainfall–runoff transformation. AFFDEF's main strength is its computational efficiency, which allows the model to perform long simulation runs (e.g. thousands of years at hourly time step). Furthermore, AFFDEF does not require extensive information in terms of historical hydrological data or geomorphology of the contributing area. It may, therefore, represent a powerful tool for performing hydrological simulation studies. The model code, written in FORTRAN programming language, provides a user friendly and ready to use tool that runs on personal computers, as well as UNIX systems. We believe that AFFDEF may represent an easy model to use and attractive instrument for hydrological applications where long simulation runs of river flows are needed at different locations of the catchment. Of particular interest is the possibility to generate river flows data in ungauged cross-sections of the watershed.

Keywords: Rainfall–runoff model; Continuous simulation; Grid based model; River flow; Calibration

Software availability

Name of the software: AFFDEF
Developer and contact address: Greta Moretti, Ingenieurbüro Winkler und Partner GmbH, Schlossstrasse 59a, D-70176 Stuttgart, Germany, Tel.: +49 711 6698727, fax: +49 711 6698720, E-mail address: moretti@iwp-online.de. Alberto Montanari, Faculty of Engineering, University of Bologna, Via del Risorgimento, 2, I-40136 Bologna, Italy, Tel.: +39 051 2093356, fax: +39 051 331446, E-mail address: alberto.montanari@mail.ing.unibo.it
Year first available: 2004
Hardware required: IBM compatible personal computer
Software required: FORTRAN compiler
Program language: FORTRAN
Program size: depending on the dimension of the investigated catchment and the length of the simulation (for instance: the executable file is 760 kb considering a matrix for the Digital Elevation Model of 84 rows × 118 columns and a length of simulation of 20 000 temporal steps)
Availability and cost: Software available at http://www.costruzioni-idrauliche.ing.unibo.it/people/alberto/affdef.html, download free of charge

1. Introduction

Spatially distributed physically based rainfall–runoff models are nowadays increasingly used for scientific and technical purposes, impact assessment studies, prediction in

* Corresponding author. Tel.: +49 711 6698727; fax: +49 711 6698720.
E-mail address: moretti@iwp-online.de (G. Moretti).

1364-8152/$ - see front matter © 2006 Elsevier Ltd. All rights reserved.
doi:10.1016/j.envsoft.2006.02.012

ungauged catchments and investigation of the spatial variability of hydrological state variables. In fact, the application of this type of model, is made easier by the increasing availability of computer power and the steadily development of geographic information systems and remote sensing techniques, which help to handle the bulk of data needed as model input. Nevertheless, the application of spatially distributed, physically based models, such as SHETRAN (Ewen et al., 2000), MIKE SHE (Refsgaard and Storm, 1995) or CASC2D (Ogden, 1997), to large catchments, is restricted by the vast amount of high quality and fine resolution data needed, in order to reliably model the physical processes taking place in the catchment (Beven, 1989).

Alternative approaches to the rainfall–runoff modelisation have, therefore, been developed, which represent physical processes with far less detail but still give a spatial distributed representation of the catchment. These models were developed to simplify the simulations of practical case studies where a detailed representation of the processes involved in the catchment is not necessary. They are distributed models where some (or all) of the hydrological processes are modelled using conceptual schemes.

Examples of these alternative models, include the SLURP (Simple LUmped Reservoir Parametric) model (Kite, 1978), which subdivides the catchment into units of different land cover and other sub-units (Grouped Response Units). It is a distributed conceptual model, which has been primarily designed in order to make use of remotely sensed data. It has been applied in climate change studies.

Another alternative model, TAC^{D} (Uhlenbrook and Sieber, 2005), is an example of a raster based conceptual model. The core of the model is a process-oriented runoff generation routine based on experimental findings, including tracer studies (Uhlenbrook et al., 2002).

Further attempts to simplify the rainfall–runoff modelling approach while maintaining a spatial description of the catchment have produced a class of semi-distributed models that make use of a distribution function to represent the spatial variability of runoff generation (Croke et al., 2006).

TOPMODEL (Beven and Kirkby, 1979) is one such model. It predicts the dynamics of the contributing areas based on the pattern of the soil topographic index. It has been applied in many practical hydrological studies such as estimation of flood frequency distribution, by continuous simulation, in ungauged catchments (Blazkova and Beven, 1997, 2002, 2004).

The HBV model of Lindström et al. (1997), whose early applications date back to the 1970s (Bergström and Forsman, 1973), belongs to the class of semi-lumped models. The authors tried to develop a model that covered the most important runoff generating processes by using the most simple and robust structure possible (Bergström, 1995). The HBV model has been applied, in several countries, for studies concerning real time forecasting, climate change impact assessment and simulations in ungauged basins.

One of the most widely used rainfall–runoff models in Australia is the Australian Water Balance Model (AWBM, Boughton, 2004; Boughton, 2006). It consists of a conceptual model that simulates the spatial variability of the saturation overland flow by means of the conceptual basis of the Antecedent Precipitation Index (API) model. In detail, a bucket with a particular storage capacity is assigned to each portion of the catchment with different storage capacity. The rainfall is abstracted until the bucket is filled, and then all rainfall becomes runoff.

The above examples show that distributed conceptual (or mixed conceptual physically based) models can be a useful tool for the solution of several practical problems related to water resources, since hydrological analyses can be performed that would not be possible by using ‘‘pure’’ lumped models. Lumped models are not capable of evaluating the effects of local land use changes (such the reduction of the permeability of urbanised areas, or the deforestation of skiing resorts) and cannot simulate river flows in internal river sections. Distributed models have the advantage, once they are calibrated by using river flow data observed at a selected site, of being able to simulate the flows in any location of the river network. Moreover, the use of conceptual schemes allows simulations that would be demanding, in terms of data requirement and computational resources, if fully physically based models were utilised.

The purpose of this article is to present the continuous simulation, spatially distributed (grid based), rainfall–runoff AFFDEF model that was developed at the University of Bologna and has recently been made available on the World Wide Web. It may be downloaded at the web site http://www.costruzioni-idrauliche.ing.unibo.it/people/alberto/affdef.html. The code is written in the FORTRAN programming language and is fully commented; it can run on a personal computer as well as a UNIX system, with a user-friendly interface.

The following requirements were determined: (a) the model simulations should be reliable in making predictions for ungauged or scarcely gauged catchments or where little information about the contributing area is available; (b) the model should allow a spatially distributed description of the geomorphological characteristics of the catchment in order to generate river flow data at any cross-section of the river network; (c) the model should perform reliable simulations of the river flows even when only short records of historical data are available; (d) the model should have some physical basis in order to constrain the range of values of some parameters by means of in situ measurements or physical reasoning and in order to decrease parameter uncertainty; (e) the model should be computationally inexpensive in such a way that long simulation runs could be performed at short time steps in a reasonably limited time, even for medium size basins.

The proposed rainfall–runoff model belongs to the class of distributed conceptual models because it allows a spatially distributed description of the catchment combined with the use of conceptual and physically based schemes for modelling hydrological processes at the grid scale. As the listed requirements show, the model has been conceived to be used for practical purposes and to be applicable to a wide spectrum of real world case studies.

The description of the model is given in the following section together with the description of the data needed to

perform rainfall–runoff simulations. The third section of the paper describes the parameters of the model and how they can be calibrated. The last section shows the application of the model to three different catchments, proving its robustness and efficiency even when limited historical information is available.

2. Description of the rainfall–runoff model

2.1. Data requirements

The model can run for any spatial resolution and for any time resolution (typically, hourly or shorter intervals). The input meteorological data consist of both observed precipitation (rainfall depths) and air temperature, at the same time step.

The input topography data are required as a grid based Digital Elevation Model (DEM), which is given in raster format by means of a $m \times n$ rectangular matrix, placed in an ASCII text file. Each element of the matrix represents the mean elevation of the corresponding DEM cell, whereas cells located outside of the catchment are assigned an elevation less than zero (e.g. −99).

To characterise the spatial pattern of the infiltration capacity, a second $m \times n$ matrix has to be provided in a separate ASCII file containing the Curve Number (CN) parameters associated to each DEM cell. The value of the CN parameter depends on soil type and land use and can be estimated by using the tables provided by the USDA (Soil Conservation Service, 1972; Young and Carleton, 2006). The soil type and land use can be found from maps, or estimated by means of in situ surveys and/or prior knowledge of the catchment. The ArcCN-Runoff tool (Zhan and Huang, 2004) is a useful ArcGIS extension that could be used for generating the Curve Number map when the maps of soil type and land use are available as shape files.

If soil type and land use data are not available at fine spatial resolution, one possible option is to lump the available data at a sub-catchment (or even catchment) scale, by assigning each sub-catchment group of cells with the same CN number (Brath and Montanari, 2000).

Finally, a $m \times n$ matrix placed in an ASCII text file is used to represent the spatial variability of the roughness on the hillslope for the overland flow. According to land use, different classes of roughness may be determined and a value for the Strickler coefficient is assigned to each class. The Strickler coefficient may be estimated from the scientific literature according to the land use type (e.g. Engman, 1986).

2.2. Identification of the flow paths

The model discretises the drainage area in square cells coinciding with the pixels of the DEM. Initially, the river network is generated from the DEM by using an existing computer code (Brath et al., 1989) which applies the D-8 method (Band, 1986; Tarboton, 1997). This approach estimates the river flow paths and the contributing area to each pixel (an example is given in Fig. 1). In detail, the river network is determined by assigning a maximum slope pointer to each DEM pixel and then processing the DEM in order to organise the river network according to the Strahler's stream ordering system (Strahler, 1964). The values of the maximum slope pointer, according to the flow direction, are shown in Fig. 2. Digital pits are filled in a pre-processing step. When pits are not located in correspondence of lakes (in this circumstance they are not eliminated), they are the result of approximations made in the discretisation of the topography from the DEM. The procedure for removing pits is generally efficient in steep basins, but may give errors in flat areas. The code stops trying to remove a pit when attempts are made to raise the original elevation of a cell above the maximum elevation of the catchment. In this case, the coordinates of the particular cell are shown on the screen and a manual adjustment of the DEM is necessary.

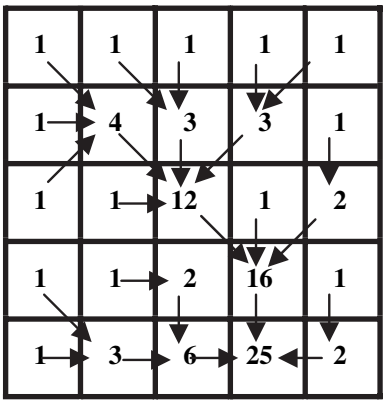

Fig. 1. Computation of the contributing area according to the flow direction.

2.3. Computation of local rainfall

The distributed approach of the model allows for spatial variation of climate input within the drainage area. Precipitation data are in the form of observed rainfall depths, linked to raingauges located within or close to the catchment. Precipitation is input to AFFDEF via an ASCII text file, listing observed precipitation in each site as well as the coordinates of each raingauge. The precipitation routine estimates rainfall, $P_l[t,(i,j)]$ (mm), as a function of time t at cell coordinates (i,j) either using Thiessen polygons or the inverse squared distance interpolation method. The Thiessen polygon method assigns to a particular cell the rainfall depth that has been recorded at the nearest raingauge at the same time step. In the second case $P_l[t,(i,j)]$ is given by the interpolation of the observed rainfall

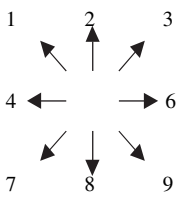

Fig. 2. Values of the maximum slope pointer indicating the flow direction.

depths $P_l[t,k]$ (mm), $k = 1,\ldots,N_R$, measured at each one of the N_R (dimensionless) raingauges, that is:

$$P_l[t,(i,j)] = \sum_{k=1}^{N_R} \lambda_k(i,j) P_l[t,k] \quad (1)$$

where the weights λ_k (dimensionless) are expressed as:

$$\lambda_k(i,j) = \frac{1/d_k^2(i,j)}{\sum_{m=1}^{N_R} 1/d_m^2(i,j)} \quad (2)$$

where $d_k(i,j)$ (m) is the distance between the (i,j) cell and the k-th raingauge. If a raingauge does not have data recorded at a particular time step, then only available measurements are taken into account by the model. The Thiessen polygons are then recalculated or the weights λ_k updated, according to the interpolation technique chosen.

2.4. Estimation of the evapotranspiration

For each DEM cell, the potential evapotranspiration is estimated using the radiation method (Doorenbos et al., 1984), which is based on a simplification of the Penman–Monteith equation. The terms related to the vapour pressure and wind speed are neglected by the radiation method as they are usually not available. Temperature is assigned to each DEM cell using Thiessen polygons, but only considering stations that have measured data at the time step t. Temperature data are input to AFFDEF by means of a ASCII text file, where the observed temperature, the coordinates of each thermometric station and the parameters of the radiation method are provided.

According to the radiation method, the evapotranspiration $E_P[t,(i,j)]$, can be expressed as a linear function of temperature at each time step t and cell of coordinates (i,j), in such a way that it can be aggregated at monthly time steps or disaggregated at short time steps without loosing the long term balance. $E_P[t,(i,j)]$ (mm month^{-1}) at the monthly step is expressed as:

$$E_P[t,(i,j)] = a + bT[t,(i,j)]N(i)W_{ta}(i) \quad (3)$$

where a (mm) and b (mm °C^{-1}) are the regression coefficients of the radiation method; $T[t,(i,j)]$ (°C) is the observed temperature at time t; $N(i)$ (dimensionless) is the monthly mean of the maximum number of daily hours of sunshine referring to the i-th month (tabulated as a function of latitude); and $W_{ta}(i)$ (dimensionless) is a compensation factor dependent upon the monthly average temperature and elevation above the sea level. $N(i)$ and $W_{ta}(i)$ can be derived according to the reference values of Tables 1 and 2 (Doorenbos et al., 1984).

Eq. (3) is therefore suitable for implementation in the model on the basis of the time step of the observed temperature data. For instance, if temperature is observed at an hourly time scale, Eq. (3) has to be divided by $24 \cdot n(i)$ to get $E_P[t,(i,j)]$ in mm h^{-1}, where $n(i)$ (dimensionless) are the number of days of the i-th month.

2.5. Computation of the local runoff response

The schematic of the hillslope hydrology simulated by AFFDEF is shown in Fig. 3. In particular, the model takes into account the evapotranspiration from the vegetation cover and the soil. The lateral sub-surface runoff and surface runoff from each hillslope cell are routed towards the basin outlet along the river network.

In order to perform continuous time simulation of the water fluxes among soil, vegetation and atmosphere, a modification of the Curve Number method (Soil Conservation Service, 1972) is used within AFFDEF as shown in Fig. 4, and described next.

AFFDEF accounts for interception of precipitation by vegetation by means of a local 'interception reservoir' at the cell (i,j), in which the rainfall depth accumulates. λ number of interception reservoirs are used, where λ is the number of

Table 1
Mean daily duration $N(i)$ of the maximum possible sunshine hours for different months and latitudes (reproduced from Table 3 in "Crop water requirements", FAO Irrigation and Drainage Paper 24)

Northern lats.	Jan	Feb	Mar	Apr	May	June	July	Aug	Sept	Oct	Nov	Dec
Southern lats.	July	Aug	Sept	Oct	Nov	Dec	Jan	Feb	Mar	Apr	May	June
50	8.5	10.1	11.8	13.8	15.4	16.3	15.9	14.5	12.7	10.8	9.1	8.1
48	8.8	10.2	11.8	13.6	15.2	16.0	15.6	14.3	12.6	10.9	9.3	8.3
46	9.1	10.4	11.9	13.5	14.9	15.7	15.4	14.2	12.6	10.9	9.5	8.7
44	9.3	10.5	11.9	13.4	14.7	15.4	15.2	14.0	12.6	11.0	9.7	8.9
42	9.4	10.6	11.9	13.4	14.6	15.2	14.9	13.9	12.6	11.1	9.8	9.1
40	9.6	10.7	11.9	13.3	14.4	15.0	14.7	13.7	12.5	11.2	10.0	9.3
35	10.1	11.0	11.9	13.1	14.0	14.5	14.3	13.5	12.4	11.3	10.3	9.8
30	10.4	11.1	12.0	12.9	13.6	14.0	13.9	13.2	12.4	11.5	10.6	10.2
25	10.7	11.3	12.0	12.7	13.3	13.7	13.5	13.0	12.3	11.6	10.9	10.6
20	11.0	11.5	12.0	12.6	13.1	13.3	13.2	12.8	12.3	11.7	11.2	10.9
15	11.3	11.6	12.0	12.5	12.8	13.0	12.9	12.6	12.2	11.8	11.4	11.2
10	11.6	11.8	12.0	12.3	12.6	12.7	12.6	12.4	12.1	11.8	11.6	11.5
5	11.8	11.9	12.0	12.2	12.3	12.4	12.3	12.3	12.1	12.0	11.9	11.8
0	12.1	12.1	12.1	12.1	12.1	12.1	12.1	12.1	12.1	12.1	12.1	12.1

Table 2
Values of the weighting factor W_{ta} at different altitudes

W_{ta} altitude [m]	Temperature [°C]																			
	2	4	6	8	10	12	14	16	18	20	22	24	26	28	30	32	34	36	38	40
0	0.43	0.46	0.49	0.52	0.55	0.58	0.61	0.64	0.66	0.71	0.73	0.75	0.77	0.78	0.85	0.82	0.83	0.84	0.85	0.86
500	0.45	0.48	0.51	0.54	0.57	0.60	0.62	0.65	0.70	0.72	0.74	0.76	0.78	0.79	0.81	0.82	0.84	0.85	0.86	0.87
1000	0.46	0.49	0.52	0.55	0.58	0.61	0.66	0.69	0.71	0.73	0.75	0.77	0.79	0.80	0.82	0.83	0.85	0.86	0.87	0.88
2000	0.49	0.52	0.55	0.58	0.61	0.64	0.66	0.69	0.71	0.73	0.75	0.77	0.79	0.81	0.82	0.84	0.85	0.86	0.87	0.88
3000	0.52	0.55	0.58	0.61	0.64	0.66	0.69	0.71	0.73	0.75	0.77	0.79	0.81	0.82	0.84	0.85	0.86	0.88	0.88	0.89
4000	0.53	0.58	0.61	0.64	0.66	0.69	0.71	0.73	0.76	0.78	0.79	0.81	0.83	0.84	0.85	0.86	0.88	0.89	0.90	0.90

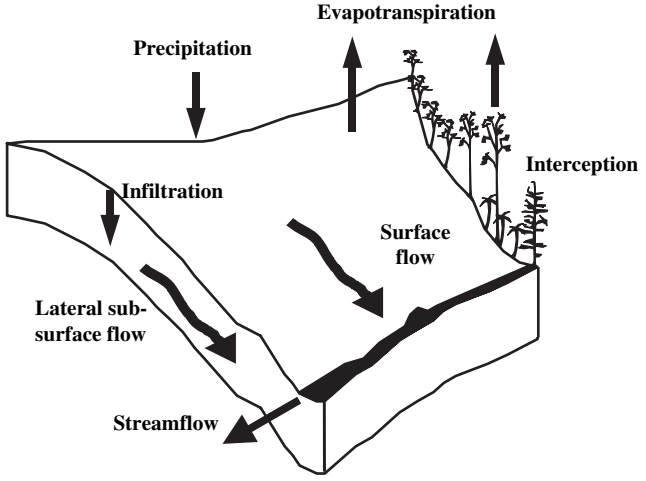

Fig. 3. Schematic of the processes of the hillslope hydrology reproduced by the model.

DEM cells used to discretise the watershed. The capacity of the interception reservoir is equal to $C_{\text{int}}S(i,j)$, where C_{int} (dimensionless) is a parameter, that is assumed to be constant over the basin and time. $S(i,j)$ (mm) is the local CN soil storativity (Soil Conservation Service, 1972; Chow et al., 1988), given by:

$$S(i,j) = 254\left(\frac{100}{\text{CN}(i,j)} - 1\right) \tag{4}$$

CN(i,j) (dimensionless) is the Curve Number at the given cell location. Once the interception reservoir is full of water, the exceeding rainfall reaches the ground, where it is split into surface and sub-surface flow. Flow subdivision is done by using an approach derived by modifying the CN equation. In detail, it is assumed that for each cell, a linear reservoir (infiltration reservoir) is located at soil level, where infiltrated water is collected. λ number of infiltration reservoirs are used. The rainfall, $P[t,(i,j)]$ (mm), that reaches the ground at the time t (i.e. overflow from the interception reservoir) is divided between surface runoff $P_n[t,(i,j)]$ (mm) and infiltrated water $I[t,(i,j)]$ (mm) according to the relationship:

$$\frac{P_n[t,(i,j)]}{P[t,(i,j)]} = \frac{F[t,(i,j)]}{HS(i,j)} \tag{5}$$

where $F[t,(i,j)]$ (mm) is the water content of the infiltration reservoir at time t. $HS(i,j)$ (mm) is the capacity of the infiltration reservoir itself, given by the parameter H (dimensionless) multiplied by the soil storativity defined in Eq. (4).

As mentioned above, the runoff response subroutine uses a modified version of the CN method to distinguish between surface runoff and infiltrated water. Since the CN method is considered as an infiltration excess process approach by many authors (see, for instance, Beven, 2000), it is expected that our proposed model is better suited for basins characterised by low permeability and prevalently impervious hillslopes, where the generation of surface runoff is more likely

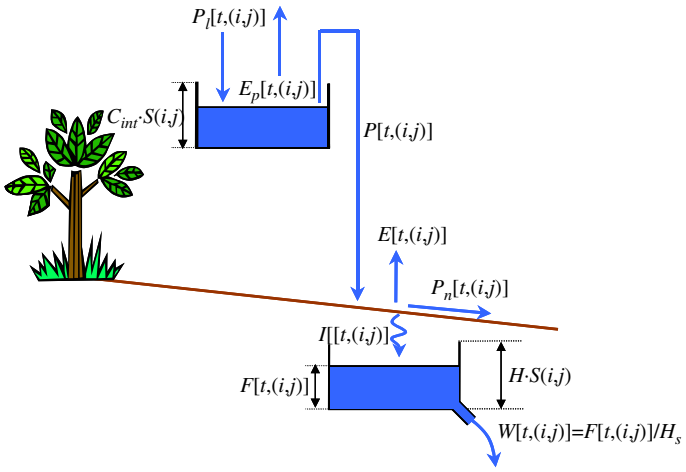

Fig. 4. Schematic representation of the model interactions among soil, vegetation and atmosphere at the local scale.

to be well represented by an excess infiltration scheme, instead of excess saturation. It should be noted that, as the capacity of the infiltration reservoir is proportional to the soil storativity S, the CN method is used to distinguish between areas having higher and lower infiltration potentials within the catchment. It is then the calibration parameter H that assigns to each cell the effective value of the infiltration storage capacity that can be derived from the hydro-pluviometric data.

The infiltrated water at time t is computed as:

$$I[t,(i,j)] = P[t,(i,j)] - P_n[t,(i,j)] \tag{6}$$

Each infiltration reservoir releases an outflow $W[t,(i,j)]$ (mm s^{-1}) to the sub-surface river network through a linear bottom discharge, according to the relationship:

$$W[t,(i,j)] = \frac{F[t,(i,j)]}{H_S} \tag{7}$$

where H_S (dimensionless) is a parameter. H and H_S are assumed to be constant with respect to both space and time.

When some water is stored in the interception reservoir, the effective evapotranspiration $E[t,(i,j)]$ (mm s^{-1}) is considered equal to $E_P[t,(i,j)]$ (mm s^{-1}, calculated as specified in Section 2.4) and is subtracted from the water content of the interception reservoir itself. When the latter is empty, or is emptied while subtracting the evapotranspiration, the remaining part of $E_P[t,(i,j)]$ is subtracted from the water content of the infiltration reservoir. In this case, it is assumed that $E[t,(i,j)]$ is varying linearly from 0 when $F[t,(i,j)] = 0$, to $E_P[t,(i,j)]$ when $F[t,(i,j)] = HS(i,j)$.

Finally, by combining the following continuity equation governing the infiltration reservoir:

$$I[t,(i,j)] - W[t,(i,j)] = \frac{\mathrm{d}F[t,(i,j)]}{\mathrm{d}t} \tag{8}$$

with the Eqs. (5)–(7) and taking the effective evapotranspiration into account, one derives the equation governing the mass balance of the infiltration reservoir, i.e.:

$$\frac{\mathrm{d}F[t,(i,j)]}{\mathrm{d}t} = -\frac{F[t,(i,j)]}{H_S} - E[t,(i,j)] + P[t,(i,j)]\left\{1 - \frac{F[t,(i,j)]}{HS(i,j)}\right\} \tag{9}$$

which is solved with the fourth order Runge–Kutta method.

2.6. The routing procedure

Surface and sub-surface flow are propagated towards the basin outlet by applying the Muskingum–Cunge model with variable parameters (Cunge, 1969). These latter are determined on the basis of the 'matched diffusivity' concept (Ponce, 1986; Orlandini and Rosso, 1996). The subroutine propagates the surface and sub-surface runoff downstream following the network ordering system determined by the slope pointers. Each cell receives water from its upslope neighbours and discharge to its downslope neighbour. For cells of flow convergence, the upstream inflow hydrograph is taken as the sum of the outflows hydrographs of the neighbouring upslope cells. Distinction between hillslope rill and network channel is based on the concept of 'constant critical support area' (Montgomery and Foufoula-Georgiou, 1993). Rill flow is therefore, assumed to occur in each cell where the upstream drainage area does not exceed the value of the calibration parameter A_0 (km^2), otherwise channel flow will occur.

2.6.1. Propagation of the surface flow

The parameters of the Muskingum–Cunge method vary in space, assuming different values on the hillslope and along the river network, and in time. In the following equations, from (10)–(19), the temporal and spatial dependence of C_1, C_2, C_3, C_4, D_n, D_h, X, c_k, B, and Q^* is omitted to simplify the notation.

The inflow and outflow discharges for a given cell of coordinates (i,j) are denoted with the subscripts in and out, respectively, and t, $t+\Delta t$ are the time steps at which they occur

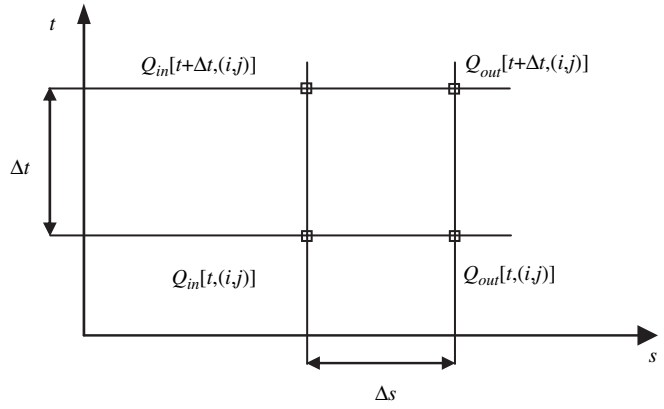

Fig. 5. Space-time grid for the resolution of the Muskingum–Cunge method for the propagation of the surface flow and the sub-surface flow.

(Fig. 5). The outflow hydrograph $Q_{\text{out}}[t+\Delta t]$ ($\text{m}^3\,\text{s}^{-1}$) from the cell is given by:

$$Q_{\text{out}}[t+\Delta t,(i,j)] = C_1 Q_{\text{in}}[t+\Delta t,(i,j)] + C_2 Q_{\text{in}}[t,(i,j)] + C_3 Q_{\text{out}}[t,(i,j)] + C_4 q_{\text{L out}}[t+\Delta t,(i,j)] \quad (10)$$

where, $Q_{\text{in}}[t+\Delta t,(i,j)]$, $Q_{\text{in}}[t,(i,j)]$ and $Q_{\text{out}}[t,(i,j)]$ are expressed in $\text{m}^3\,\text{s}^{-1}$. $q_{\text{L out}}[t+\Delta t,(i,j)]$ ($\text{m}^3\,\text{s}^{-1}\,\text{m}^{-1}$) is the lateral inflow rate expressed by:

$$q_{\text{L out}}[t+\Delta t,(i,j)] = P_n[t,(i,j)]\frac{\Delta x \Delta y}{\Delta s}\frac{1}{1000} \quad (11)$$

where $P_n[t,(i,j)]$ (mm) is the surface runoff (local net rainfall that reaches the ground, see Section 2.5), Δx (m) and Δy (m) are the dimension of the cell in the horizontal and vertical direction, respectively, Δs (m) is the channel length within the cell. C_1 (dimensionless), C_2 (dimensionless), C_3 (dimensionless) and C_4 (m) are the time and space variable routing coefficients expressed by the following relationships:

$$C_1 = \frac{c_k(\Delta t/\Delta s) - 2X}{2(1-X) + c_k(\Delta t/\Delta s)} \quad (12)$$

$$C_2 = \frac{c_k(\Delta t/\Delta s) + 2X}{2(1-X) + c_k(\Delta t/\Delta s)} \quad (13)$$

$$C_3 = \frac{2(1-X) - c_k(\Delta t/\Delta s)}{2(1-X) + c_k(\Delta t/\Delta s)} \quad (14)$$

$$C_4 = \frac{2c_k\Delta t}{2(1-X) + c_k(\Delta t/\Delta s)} \quad (15)$$

where Δt (s) is the time interval and c_k ($\text{m}\,\text{s}^{-1}$) is the kinematic celerity. X (dimensionless) is a weighting factor, which is introduced to match the numerical diffusion coefficient of the Muskingum model, $D_n = c_k\Delta s(1/2 - X)$ ($\text{m}^2\,\text{s}^{-1}$) and the hydraulic diffusivity of the convection–diffusion flow equation, $D_h = Q^*/2Bi_f$ ($\text{m}^2\,\text{s}^{-1}$) (Cunge, 1969). X is expressed by:

$$X = \frac{1}{2}\left(1 - \frac{Q^*}{Bc_k i_f \Delta s}\right) \quad (16)$$

while c_k is computed from the Gauckler–Strickler formula assuming rectangular river cross-section:

$$c_k = k_s i_f^{1/2} B^{2/3}(w+2)^{-5/3}\left(\frac{5}{3}w + 2\right) \quad (17)$$

where k_s ($\text{m}^{1/3}\,\text{s}^{-1}$) is the Gauckler–Strickler roughness, i_f (dimensionless) is the friction slope and w (dimensionless) is the width/depth ratio of the water surface. The assumption of a rectangular river cross-section is frequently adopted in spatially distributed models (Orlandini and Rosso, 1996) and can be considered reasonable for river sections where the width of the surface water is much greater than the water depth. In the case of rill flow, which typically occurs on the hillslopes, the assumption of a rectangular section is a conceptual approximation. Here the width/depth ratio of the water surface and roughness of the hillslopes are considered calibration parameters. When the Muskingum–Cunge model is applied to hillslopes, the literature reports much higher values for w and lower values for k_s with respect to river network applications.

The width of the water surface B (m) can be estimated by applying the Gauckler–Strickler equation:

$$B = \left[\frac{Q^*(w+2)^{2/3}w}{k_s i_f^{1/2}}\right]^{3/8} \quad (18)$$

where Q^* ($\text{m}^3\,\text{s}^{-1}$) a first order estimation of the river flow, given by the relationship (Ponce and Yevjevich, 1978):

$$Q^* = \frac{1}{3}\{Q_{\text{in}}[t,(i,j)] + Q_{\text{in}}[t+\Delta t,(i,j)] + Q_{\text{out}}[t,(i,j)]\} \quad (19)$$

As X varies in space and time with flow, the numerical diffusivity simulates the hydraulic diffusivity of the actual flood wave. The diffusion wave model is unconditionally stable since numerical instabilities, which may arises when $D_n < 0$ ($X > 1/2$), are prevented by matching the numerical and hydraulic diffusivities.

On the hillslope, w has a constant value with respect to both space and time, whereas the Strickler roughness (which is constant in time) is evaluated for each cell on the basis of land use. Along the river network, w is assumed constant in space and time, but assumes a different value with respect to the hillslope; the channel roughness is allowed to vary from a minimum to a maximum value depending on the elevation according to the relationship:

$$k_s = k_{\text{sr}}^1 \exp\left[\frac{\log\left(k_{\text{sr}}^0/k_{\text{sr}}^1\right)}{\left(z_{\text{top}} - z_{\text{outlet}}\right)}(z(i,j) - z_{\text{outlet}})\right] \quad (20)$$

where k_{sr}^0($\text{m}^{1/3}\,\text{s}^{-1}$) and k_{sr}^1($\text{m}^{1/3}\,\text{s}^{-1}$) are the maximum and minimum Strickler roughness for the channel network, $z(i,j)$ (m) is the elevation of the cell (i,j), z_{top} (m) and z_{outlet} (m)

are the maximum elevation of the catchment and the elevation of the outlet, respectively.

2.6.2. Propagation of the sub-surface flow

The outflow from the infiltration reservoir $W[t,(i,j)]$ locally feeds the flow along the sub-surface river network. Let us suppose that the sub-surface flow Q_s' ($m^3\,s^{-1}$) reaches a cell of the channel network of coordinates (i',j') at time t'. Q_s' is then joined to the surface flow of the cell of coordinates (i',j') at time t'.

Again, the propagation of the sub-surface flow, is modelled with the Muskingum model according to the following equation:

$$Q_{\text{out}}^{\text{sub}}[t+\Delta t,(i,j)] = C_1^{\text{sub}} Q_{\text{in}}^{\text{sub}}[t+\Delta t,(i,j)] + C_2^{\text{sub}} Q_{\text{in}}^{\text{sub}}[t,(i,j)] + C_3^{\text{sub}} Q_{\text{out}}^{\text{sub}}[t,(i,j)] + C_4^{\text{sub}}\left(\frac{W[t,(i,j)]\Delta x\Delta y}{1000\Delta s}\right) \quad (21)$$

where $Q_{\text{in}}^{\text{sub}}$($m^3\,s^{-1}$) and $Q_{\text{out}}^{\text{sub}}$($m^3\,s^{-1}$) are the inflow and outflow discharges for a given cell, and $W[t,(i,j)]$ ($mm\,s^{-1}$) is the outflow from the infiltration reservoir. The routing parameters for the sub-surface flow C_1^{sub} (dimensionless), C_2^{sub} (dimensionless), C_3^{sub} (dimensionless) and C_4^{sub} (m) are expressed as the following (note that the temporal and spatial dependence of C_1^{sub}, C_2^{sub}, C_3^{sub}, C_4^{sub}, X^{sub}, c_k^{sub}, $Q^{*\text{sub}}$ and D_h^{sub} is omitted to simplify the notation):

$$C_1^{\text{sub}} = \frac{c_k^{\text{sub}}(\Delta t/\Delta s) - 2X^{\text{sub}}}{2\left(1-X^{\text{sub}}\right) + c_k^{\text{sub}}(\Delta t/\Delta s)} \quad (22)$$

$$C_2^{\text{sub}} = \frac{c_k^{\text{sub}}(\Delta t/\Delta s) + 2X^{\text{sub}}}{2\left(1-X^{\text{sub}}\right) + c_k^{\text{sub}}(\Delta t/\Delta s)} \quad (23)$$

$$C_3^{\text{sub}} = \frac{2\left(1-X^{\text{sub}}\right) - c_k^{\text{sub}}(\Delta t/\Delta s)}{2\left(1-X^{\text{sub}}\right) + c_k^{\text{sub}}(\Delta t/\Delta s)} \quad (24)$$

$$C_4^{\text{sub}} = \frac{2c_k^{\text{sub}}\Delta t}{2\left(1-X^{\text{sub}}\right) + c_k^{\text{sub}}(\Delta t/\Delta s)} \quad (25)$$

c_k^{sub} ($m\,s^{-1}$) and X^{sub} (dimensionless) are the kinematic celerity and the weighting factor for the sub-surface flow. c_k^{sub} and X^{sub} have different formulae (Orlandini et al., 1999) with respect to the corresponding variables introduced for surface flow. In particular, the sub-surface kinematic celerity c_k^{sub}, which varies spatially, is given by Darcy's law:

$$c_k^{\text{sub}} = K_{\text{sat}} i_s \quad (26)$$

In Eq. (26), K_{sat} ($m\,s^{-1}$) is the saturated conductivity of the soil and i_s (dimensionless) is the slope of the sub-surface river network, which is assumed to be equal to the surface river network. This is the first major simplification used in the model. K_{sat} defines the velocity of the sub-surface flow and can be estimated based on the characteristics of the soil or, alternatively, can be treated as a calibration parameter constant in space and time.

The weighting factor X^{sub} varies in space and time and is computed according to the relationship:

$$X^{\text{sub}} = \frac{1}{2} - \frac{Q^{*\text{sub}}}{i_s B_P^{\text{sub}} c_k^{\text{sub}} \Delta s} \quad (27)$$

where $Q^{*\text{sub}}$ ($m^3\,s^{-1}$) is a reference sub-surface flow, analogous to Q^* for the surface network and computed in the same manner (see Eq. (19)). B_P^{sub} (m) is the width of the water surface, which can be treated as a calibration parameter constant in space and time, assuming a rectangular cross-section for the sub-surface river network.

Eq. (27) is again derived by matching the numerical diffusion coefficient of the Muskingum–Cunge method, D_n^{sub} ($m^2\,s^{-1}$), with the hydraulic diffusivity of the sub-surface flow D_h^{sub} ($m^2\,s^{-1}$), expressed by:

$$D_h^{\text{sub}} = Q^{*\text{sub}} / \left(i_s B_p^{\text{sub}}\right) \quad (28)$$

D_h^{sub} varies in space and time. As one may note, the sub-surface flow is modelled as a unique entity, without any distinction between near surface and deep water flow. This simplified description has the advantage of reducing the number of the model parameters and, consequently, also the amount of historical data required for calibration. However, a significant approximation in simulations of low discharges is expected, especially in highly permeable basins.

2.6.3. The accuracy of the Muskingum–Cunge method

The Muskingum–Cunge method used for the propagation of the surface flow is based on the algebraic linear equation shown in Eq. (10). This is solved by means of the diffusion wave scheme, allowing rapid computation of flow in each section of the drainage network. Ponce (1986) showed that the diffusion wave method gives an accurate and stable solution, which is not affected by the resolution of the cell. To ensure the accuracy of the method, the scientific literature recommends respecting the empirical condition:

$$C_1 \geq 0 \quad (29)$$

whereas C_2 and C_3 can assume negative values without affecting the accuracy of the method (Ponce and Theurer, 1982). Condition (29) is verified if and only if:

$$C_u + \delta \geq 1 \quad (30)$$

where $C_u = c_k\,\Delta t/\Delta s$ (dimensionless) is the Courant number and $\delta = 1 - 2X$ (dimensionless). In such case that condition (30) is not verified, as may happen for the overland flow, especially in upland areas (Orlandini and Rosso, 1996), the following condition is forced in the model:

$$\delta = 1 - C_u \quad (31)$$

from which the value of δ is derived for the computation of X. As observed by Orlandini and Rosso (1996) and as demonstrated by testing the model, condition (31) improves the accuracy of the scheme without modifying the features of the catchment response.

The forcing conditions given in Eqs. (29)–(31) are also used in solving the Muskingum–Cunge equation (21) for the propagation of the sub-surface flow. In this case, the condition of accuracy (29) is expressed in terms of C_1^{sub} and the Courant number is computed using c_k^{sub}.

3. Model calibration

The parameters of the model are listed in Table 3. The values of some parameters, namely A_0, k_{sr}^0, k_{sr}^1 and w_r and the values of the Strickler coefficients for the different classes of roughness on the hillslope, can be estimated by physical reasoning or in situ measurements ('estimated' values shown in Table 3). In particular, the value of A_0 is usually identified by comparing the river network determined by the model with a topography map of the catchment showing the natural flow paths. As an initial estimate one may set $A_0 = 0.5\ \mathrm{km}^2$. A first trial value for k_{sr}^0, k_{sr}^1 and w_r along the river network can be derived from the analysis of the river network geometry. The parameter C_{int} is not well correlated with the other parameters but can be calibrated separately by comparing observed values of the runoff coefficient with estimates derived by simulating sufficiently long records of synthetic river flows. The remaining parameters can be calibrated manually with a trial and error procedure by comparing observed and simulated hydrographs. A sensitivity analysis carried out by Brath et al. (2004) is useful in guiding the user in tuning the model parameters. It was found that certain input parameters had a more direct effect on the model outputs than others did. For example, the parameters of the surface Muskingum model (w_v, k_{sv}, w_r, k_{sr}^0, k_{sr}^1) mainly affect peak flow timing and somewhat affect hydrograph shape and peak flow magnitude. The parameters that refer to hillslopes (w_v, k_{sv}) have a more significant influence on the simulated river flows than the river network parameters, especially if A_0 is not small. The infiltration reservoir parameters H and H_{s} have a large effect on peak flow magnitude. Finally, the parameter H_{s} and those of the sub-surface Muskingum model $\left(K_{\mathrm{sat}}, B_P^{\mathrm{sub}}\right)$ have an effect on the recessing limb of the hydrograph.

A routine for performing automatic calibration, which makes use of the Shuffled Complex Evolution (SCE, Duan et al., 1992) global optimisation algorithm, was included in the AFFDEF code. The user must select the parameters to be automatically calibrated, and define their lower and upper bounds. The automatic calibration procedure, using a least square objective function, results in a better agreement between observed and simulated flows. This procedure, however, is computationally demanding, especially when dealing with very large watersheds (Boughton, 2006).

4. Examples of AFFDEF application

A number of applications of AFFDEF can be already found in the scientific literature (Brath and Montanari, 2000; Brath et al., 2001, 2002, 2003, 2004; Montanari and Brath, 2004). In Brath et al. (2004), the Reno River Basin in Italy was used to study the reliability of the model when it was calibrated using data sets of increasing length. Overall, the results indicate that the best out-of-sample performances are obtained by calibrating the model with minimum periods of 3 months. This seems to be an improvement over the requirement of a calibration period of at least 1 year for lumped models.

Table 3
Rainfall–runoff model input parameters and their values. The values were partly optimised by calibration (calibrated) and partly estimated by in situ measurements or physical reasoning (estimated)

Parameter	Dimension and symbol	Method of estimation	Upper Neckar	Samoggia River	Le Loup River
Channel width/height ratio for the hillslope	w_v (dimensionless)	Calibrated	92 949	600	600
Strickler coefficients for the N-classes of roughness on the hillslope	$k_{\mathrm{sv}}(\mathrm{i})$, $i = 1,N$ ($\mathrm{m}^{1/3}\ \mathrm{s}^{-1}$)	Estimated	5.0, 43.1, 6.1, 5.9[a]	0.5[b]	0.1[b]
Channel width/height ratio for the channel network	w_r (dimensionless)	Estimated	20	20	20
Maximum and minimum Strickler roughness for the channel network	k_{sr}^0, k_{sr}^1 ($\mathrm{m}^{1/3}\ \mathrm{s}^{-1}$)	Estimated	6–10	10–25	10–22
Value of the Curve Number for each cell	CN (dimensionless)	Estimated	–	–	–
Constant critical source area	A_0 (km^2)	Estimated	20.9	0.5	10.5
Saturated hydraulic conductivity	K_{sat} ($\mathrm{m\ s}^{-1}$)	Calibrated	0.099	0.01	0.01
Width of the rectangular cross-section of the sub-surface water flow	B_P^{sub}(m)	Calibrated	0.5	0.5	0.5
Bottom discharge parameter for the infiltration reservoir capacity	H_{S} (s)	Calibrated	390 595	79 000	80 000
Multiplying parameter for the infiltration reservoir capacity	H (dimensionless)	Calibrated	0.40	0.08	0.40
Multiplying parameter for the interception reservoir capacity	C_{int} (dimensionless)	Calibrated	0.13	0.65	0.20

[a] $N = 4$.
[b] $N = 1$.

Brath et al. (2002) used the model for estimating the flood frequency distribution of the Samoggia River basin, located in northern Italy. The model proved to be robust in the simulation of the observed flood frequency distribution, even if only short historical rainfall, temperature and river flows record were available for model calibration. An example of the success of the model in investigating the effects of land use change on flood flows may be found in Brath et al. (2003).

In the following section, three applications of AFFDEF are presented. The first test-site considered is the 1200-km^2 Upper Neckar catchment, located in the South-west of Germany. The model was calibrated using 13 months of observed discharges and then validated over a period of 10 years. The second and third examples are used to show the performance of the model when it is calibrated using a limited historical data. The Samoggia River basin and the Loup River basin located in southern France are used as the test-sites in these examples.

The performance of the model was assessed by means of the following goodness-of-fit-indicators:

(i) Efficiency according to Nash–Sutcliffe (Nash and Sutcliffe, 1970):

$$\text{N.S.} = 1 - \frac{(Q_{\text{sim}} - Q_{\text{obs}})^2}{(Q_{\text{obs}} - \overline{Q_{\text{obs}}})} \tag{32}$$

(ii) Relative accumulated difference

$$\text{R.A.D.} = \frac{\sum Q_{\text{sim}} - \sum Q_{\text{obs}}}{\sum Q_{\text{obs}}} \tag{33}$$

(iii) Peak relative error

$$\text{P.E.} = \frac{(\overline{Q_{\text{sim}}})_{\max} - (\overline{Q_{\text{obs}}})_{\max}}{(\overline{Q_{\text{obs}}})_{\max}} \tag{34}$$

where Q_{sim} and Q_{obs} are the simulated and observed discharge, $\overline{Q_{\text{obs}}}$ is the mean observed discharge and $(\overline{Q_{\text{sim}}})_{\max}$ and $(\overline{Q_{\text{obs}}})_{\max}$ are the mean of the maximum annual simulated and observed discharge.

The computed goodness-of-fit indicators for the three applications are given in Table 4 for the validation period. The three applications of AFFDEF to the three catchments are described next.

Table 4
Performance of the model in the validation phase for the different case studies

Case-study	Validation		
	Nash–Sutcliffe	Relative accumulated difference	Peak error
Upper Neckar	0.72	−0.054	0.002
Samoggia	0.69	−0.066	0.063
Le Loup	0.74	−0.566	0.175

4.1. The Upper Neckar catchment

The Upper Neckar catchment close to the Horb gauging station covers an area of 1200 km^2. The boundary of the catchment is bordered by the Black Forest in the South-west and the Schwäbische Alb in the South and South-east. The main stream is around 61.5 km in length, whilst the elevation in the catchment ranges from 380 to 1000 m above sea level (a.s.l.). Coniferous trees are the most dominant vegetation, especially in the western area. The mean annual runoff at the Horb outlet is 14.87 m^3/s. For the topography input, a 30 m resolution DEM was used, which was resampled at a 1 × 1 km^2 scale. This resolution is the one adopted in the model. A map of the Curve Number (CN) is required as input, to characterise the spatial pattern of the infiltration capacity of the drainage area. The CN value depends on the soil type and land use, and was estimated using tables provided by the USDA (Soil Conservation Service, 1972). This information was extracted from soil and land use maps provided by the State Institute for Environmental Protection (LfU, Baden-Württemberg).

Daily precipitation and daily mean air temperature data were obtained from the German Weather Service. The external Drift Kriging method (Ahmed and de Marsily, 1987) was used to produce spatially distributed precipitation and temperature data at a 1 × 1 km^2 grid resolution. As temperature showed a fairly constant lapse rate, topographic elevation was used as the drift variable for interpolating temperature. In contrast, the rate of change of the precipitation becomes lower for higher elevations, therefore the square root of the topographic elevation was assumed to be a suitable approximation of such variation and it was therefore used as the drift variable for precipitation.

4.1.1. Model calibration and validation

The mean daily discharge data at the Horb station were also obtained from LfU, Baden-Württemberg. These data were used to automatically calibrate the model, from 15 June 1961 to 31 July 1962, by means of the SCE global optimisation algorithm. The objective function to be minimized was the squared difference between the observed discharge and the simulated discharge. Table 3 lists the values of the calibrated and estimated parameters. Finally AFFDEF was run from 15 June 1963 to 31 December 1974, (validation period) and the simulated river flows were compared to the observed discharge at Horb. Fig. 6a compares the simulated and observed hydrographs for the 1-year calibration period, whilst Fig. 6b shows a scatterplot of simulated versus observed discharge for the validation period. From the scatterplot and the goodness-of-fit indicators listed in Table 4, it can be concluded that the model reproduced the recorded discharge, at the Horb cross-section, quite well.

4.2. Samoggia River basin

A full description of the Samoggia River is presented in Brath et al. (2002). The Samoggia River flows from South to North, in the Apennines Mountains, near the city of Bologna. It is a left bank tributary to the Reno River. The total area of the basin, up to Calcara is 178 km^2 (river flows in the upper

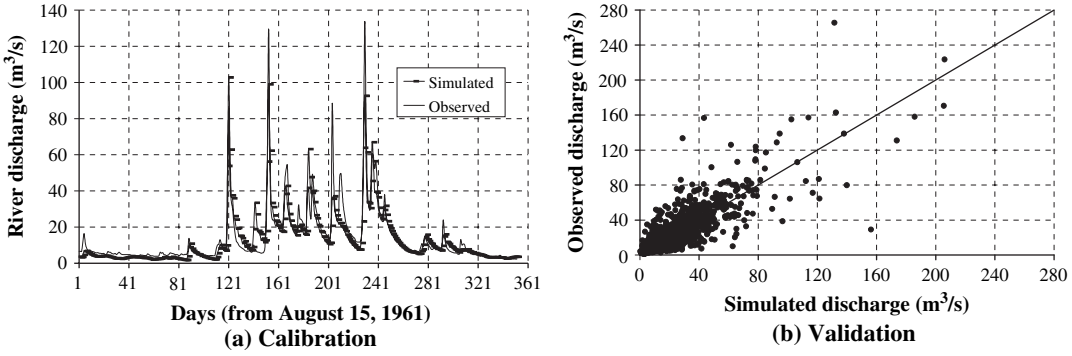

Fig. 6. Application to the Upper Neckar. (a) Comparison between observed and simulated calibration hydrographs (b) Scatterplots of the simulated discharge versus the corresponding observed values for the validation period.

part of the catchment, up to Calcara, are simulated in this study). The catchment is generally mountainous with a maximum altitude of 850 m a.s.l. The main stream is 60 km in length. The mountainous areas consist of soils and rocks of sedimentary origin, covered by broad-leaved woods, and are characterised by a low permeability which tends to decrease with increasing altitude. In contrast, the lower part of the basin consists of highly permeable alluvial fans and is covered by farmlands and urbanised areas (the latter occupying less than the 5% of the total basin area). Because of their low permeability and remarkably extension with respect to the total catchment surface, mountain areas contribute in a considerable way to the formation of the flows, which are mainly generated as infiltration excess runoff.

The topography of Samoggia River basin is described by a 250 × 250 m Digital Elevation Model. The hillslopes are significantly steep, with 44% of the area having slopes between 10% and 20%. An extensive database of soil texture, relative permeability and organic content has been derived from a 1:250.000 scale digital soil map, provided by the local administration. Meteorological data consist of hourly rainfall observed in three raingauges over the basin, during the four-year period of 1994–1997. In addition, hourly temperature data recorded at one site in the watershed and historical data of hourly river discharges recorded at Calcara are available over the same time period.

4.2.1. Model calibration and validation

For the Samoggia River, AFFDEF was manually calibrated by comparing observed and simulated river flows, observed for one flood event that occurred on October 8, 1996. We deliberately chose a short calibration data set in order to mimic a situation where data are scarce, such as in scarcely gauged basins. The same methodology was applied to the Le Loup River case study described in the following section.

The parameter A_0 was set to 0.5, by experience obtained in previous applications and by verifying the blue lines of the resulting river network. Parameter C_{int} was calibrated by comparing observed and simulated runoff coefficients. w_r, k_{sr}^0, k_{sr}^1 were fixed on the basis of prior knowledge of the river network, while K_{sat} was set to a physically reasonable value with respect to the soil type in the watershed. The remaining parameters (w_v, k_{sv}, H, H_{s} and B_P^{sub}) were manually tuned. Table 3 reports all the parameters values used in this study. Fig. 7 shows observed and simulated flood hydrographs for the calibration event, while Fig. 8 shows a scatterplot of observed versus simulated river flows for the entire 1994–1997 period. This can be considered a validation period, since the calibration event included only a small part of the data. The Nash coefficient of efficiency (Table 4) is equal to 0.69. This fit can be considered to be quite good, in view of the limited amount of data used for model calibration.

4.3. Le Loup River basin

Le Loup River is one of the case studies selected in the MOPEX research project, in order to provide an extended database to be used for comparing different approaches to rainfall–runoff modelling. An extended database for the Loup River, and other 39 rivers in France, was provided by Meteofrance.

The Le Loup River flows from the Montagne de l'Audibergue in the West, to the Mediterranean Sea in the East, into which discharges between the cities of Nice and Antibes. The total area of the basin up to Villeneuve, is 288 km^2 (river flows in the upper part of the catchment, up to Villeneuve, are simulated in this study). The drainage basin consists mainly of mountainous areas; the maximum altitude is 1753 m a.s.l., while the main stream is about 45 km in length.

The topography of Le Loup River basin is described by a 300 × 300 m DEM. The hillslopes are, again, considered quite steep, since 30% of the DEM cells have slopes between 10% and 20%. As mentioned previously, a database of soil type and land use was provided by Meteofrance. The available meteorological data consist of hourly rainfall observed in one raingauge in the basin, from 1 January, 1999, to 31 July, 2002. Hourly temperature data recorded at one site in the watershed and historical data of hourly river discharges recorded at Villeneuve are also available over the same time period.

4.3.1. Model calibration and validation

AFFDEF was calibrated manually, for the Le Loup River, by using the same optimisation procedure described above for the Samoggia River. Calibration was performed by

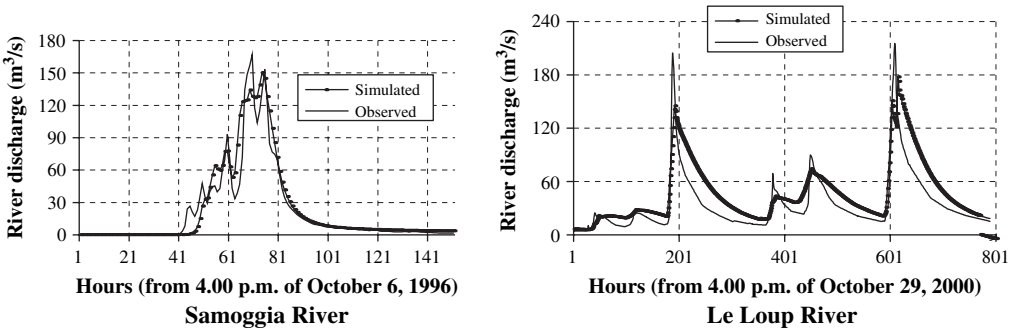

Fig. 7. Calibration of AFFDEF on a single flood event for Samoggia and Le Loup rivers. Comparison between observed and simulated calibration hydrographs.

comparing observed and simulated river discharges of the high flow event that occurred on 24 November 2000. Fig. 7 shows observed and simulated flood hydrographs for the calibration event, while Fig. 8 shows a scatterplot of observed versus simulated river flows for the period 1 January 1999, to 31 July 2002 (the calibration event is a negligible fraction of the validation period). The efficiency according to the Nash–Sutcliffe coefficient is 0.74 (Table 4). The resulting parameter values are reported in Table 3.

It is interesting to note that many calibrated and estimated input parameters for the Samoggia River and Le Loup River, are similar. This result is to be expected, since the two watersheds are quite similar. The most significant differences are found in the critical source area, A_0, and the interception and infiltration parameters, C_{int} and H. These are essentially conceptual parameters and it is, therefore, difficult to identify a physical explanation for their values. They could, in fact, compensate for approximations made within AFFDEF, which may have different effects in different catchments.

A possible justification for the lower value of the critical source area in the Samoggia watershed could be the presence of very steep hillslopes, whilst the high value of the interception parameter could be caused by the small value of the runoff coefficient (about 0.45). AFFDEF assumes therefore that a significant part of rainfall is lost as interception. Finally, the small value of the infiltration parameter, for the Samoggia River, might be due to the presence of a very rapid response to rainfall, which implies a rapid decrease of the recessing limb of the hydrographs.

The similarity in value of many AFFDEF parameters shows that the model is robust and that it can be calibrated with a quick optimisation exercise. It is the subject of on going work, to try to relate such parameters to the physical behaviours of the investigated watershed.

5. Concluding remarks

This paper has presented a rainfall–runoff model that was recently made public via the World Wide Web (http://www.costruzioni-idrauliche.ing.unibo.it/people/alberto/affdef.html). The model, called AFFDEF, is spatially distributed (grid based) and can perform continuous time simulation of river flows at any time step and any location in a watershed. The model was optimised in order to reduce computation time: for example, the present version of AFFDEF is able to generate one thousand of years of hourly river flow data, for the applications considered here, in about 24 h. AFFDEF could, therefore, be a useful tool for performing spatially distributed hydrological simulation studies. The originality of AFFDEF lies in the proposed concepts and simplifications of the processes that allow the calibration of the model in situations where limited data are available.

Three applications of AFFDEF are presented here, with reference to three river basins located in Germany, Italy and France. In the last two applications, the distributed model proved to be robust and efficient, even though it was calibrated using limited historical data.

AFFDEF was made computationally efficient by using simplified representations of some hydrological processes. In

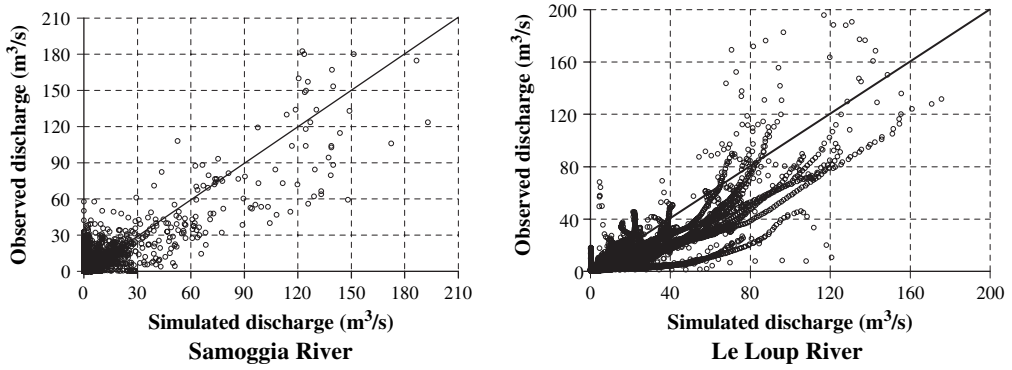

Fig. 8. Validation of AFFDEF for Samoggia and Le Loup rivers. Validation periods are 1994–1997 for Samoggia and 1 January 1999, to 31 July 2002, for Le Loup.

particular, the sub-surface flows are modelled using a simple approach (see Section 2.5), which does not distinguish between near surface and deep groundwater fluxes. This approximation might result in significant imprecision in the modelling of the recessing limb of the hydrograph, especially in the case of highly permeable and flat river basins.

Acknowledgements

AFFDEF was developed thanks to the co-operation and suggestions of many colleagues and students, to whom we are very grateful. Comments from two anonymous referees lead to a substantial improvement of the paper. The study presented here is a part of the researches carried out by the Working Group of the University of Bologna of the Prediction in Ungauged Basins initiative of the International Association of Hydrological Sciences. The work has been partially supported by the Italian National Research Council – Group for the Prevention of Hydrogeological Disasters (contract n.01.01014.PF42) and by the Italian Government through its national grant to the program on ''Hydrological Safety of Impounded Rivers''. The authors wish to thank the Institute of Hydraulic Engineering (IWS) of the University of Stuttgart (Germany) for providing the data of the Upper Neckar. The data set for Le Loup River was provided by Meteofrance.

References

Ahmed, S., de Marsily, G., 1987. Comparison of geostatistical methods for estimating transmissivity using data on transmissivity and specific capacity. Water Resources Research 23 (9), 1717–1737.

Band, L.E., 1986. Topographic partition of watersheds with digital elevation models. Water Resources Research 22, 15–24.

Bergström, S., 1995. The HBV model. In: Singh, V.P. (Ed.), Computer Models of Watershed Hydrology. Water Resource Publications, Highlands Ranch, CO.

Bergström, S., Forsman, A., 1973. Development of a conceptual deterministic rainfall–runoff model. Nordic Hydrology 4, 147–170.

Beven, K.J., 1989. Changing ideas in hydrology: the case of physically-based models. Journal of Hydrology 105, 157–172.

Beven, K.J., 2000. Rainfall–Runoff Modelling. Wiley, London.

Beven, K.J., Kirkby, M.J., 1979. A physically based, variable contributing area model of basin hydrology. Hydrological Science Bulletin 24 (1), 43–69.

Blazkova, S., Beven, K.J., 1997. Flood frequency prediction for data limited catchments in the Czech Republic using a stochastic rainfall model and TOP-MODEL. Journal of Hydrology 195, 256–278.

Blazkova, S., Beven, K.J., 2002. Flood frequency estimation by continuous simulation for a catchment treated as ungauged (with uncertainty). Water Resources Research 38 (8), doi:10.1029/2001WR000500.

Blazkova, S., Beven, K.J., 2004. Flood frequency estimation by continuous simulation of subcatchment rainfalls and discharges with the aim of improving dam safety assessment in a large basin in the Czech Republic. Journal of Hydrology 292, 153–172.

Boughton, W., 2004. The Australian water balance model. Environmental Modelling & Software 19 (10), 943–956.

Boughton, W., 2006. Calibrations of a daily rainfall–runoff model with poor quality data. Environmental Modelling & Software 21 (8), 1114–1128.

Brath, A., La Barbera, P., Mancini, M., Rosso, R., 1989. The use of distributed rainfall–runoff models based on GIS at different scales of information, Hydraulic Engineering 1989. In: Proceedings of the National Conference on Hydraulic Engineering August 1989. ASCE, New Orleans, USA, 14–18 August 1989.

Brath, A., Montanari, A., 2000. Effects of the spatial variability of soil infiltration capacity in distributed rainfall–runoff modelling. Hydrological Processes 14 (5), 2779–2794.

Brath, A., Montanari, A., Toth, E., 2001. Comparing the calibration requirements and the simulation performances of lumped and distributed hydrological models: an Italian case study. Eos. Trans. AGU 82, Spring Meet. Suppl., Abstract: H31D-04.

Brath, A., Montanari, A., Moretti, G., 2002. On the use of simulation techniques for the estimation of peak river flows. In: Proceedings of the International Conference on Flood Estimation, Berna, 6–8 March 2002, Rep II-17. CHR/KHR, International Commission for the Hydrology of the Rhine basin, Lelystad, Netherlands, pp. 587–599.

Brath, A., Montanari, A., Moretti, G., 2003. Assessing the effects on flood risk of the land-use changes in the last five decades: an Italian case study. IAHS Publication 278, 435–441.

Brath, A., Montanari, A., Toth, E., 2004. Analysis of the effects of different scenarios of historical data availability on the calibration of a spatially-distributed hydrological model. Journal of Hydrology 291, 272–288.

Chow, V.T., Maidment, D.R., Mays, L.W., 1988. Applied Hydrology. McGraw-Hill, Singapore.

Croke, B.F.W., Andrews, F., Jakeman, A.J., Cuddy, S.M., Luddy, A., 2006. IHACRES classic plus: a redesign of the IHACRES rainfall–runoff model. Environmental Modelling & Software 21 (3), 426–427.

Cunge, J.A., 1969. On the subject of a flood propagation computation method (Muskingum method). Journal of Hydraulic Research 7, 205–230.

Doorenbos, J., Pruitt, W.O., Aboukhaled, A., Damagnez, J., Dastane, N.G., Van der Berg, C., Rijtema, P.E., Ashford, O.M., Frere, M., 1984. Guidelines for Predicting Crop Water Requirements. FAO Irrigation and Drainage Paper, Rome.

Duan, Q., Sorooshian, S., Gupta, V., 1992. Effective and efficient global optimization for conceptual rainfall–runoff models. Water Resource Research 28 (4), 1015–1031, doi:10.1029/91WR02985.

Engman, E.T., 1986. Roughness coefficients for routing surface runoff. Journal of Irrigation and Drainage Engineering – ASCE 112, 39–53.

Ewen, J., Parkin, G., O'Connell, P.E., 2000. SHETRAN: distributed river basin flow and transport modeling system. In: Proceedings of the American Society of Civil Engineering. Journal of Hydrologic Engineering 5, 250–258.

Kite, G.W., 1978. Development of a hydrologic model for a Canadian watershed. Canadian Journal of Civil Engineering 5 (1), 126–134.

Lindström, G., Johansson, B., Persson, M., Gardelin, M., Bergström, S., 1997. Development and test of the distributed HBV-96 hydrological model. Journal of Hydrology 201, 272–288.

Montanari, A., Brath, A., 2004. A stochastic approach for assessing the uncertainty of rainfall–runoff simulations. Water Resources Research 40 (1), W01106, doi:10.1029/2003WR002540.

Montgomery, D.R., Foufoula-Georgiou, E., 1993. Channel network source representation using digital elevation models. Water Resources Research 29 (12), 3925–3934, doi:10.1029/93WR02463.

Nash, J.E., Sutcliffe, J.V., 1970. River flow forecasting through conceptual models. Part I. A discussion of principles. Journal of Hydrology 10, 282–290.

Ogden, F.L., 1997. CASC2D Reference Manual. Department of Civil & Environmental Engineering, University of Connecticut, Storrs.

Orlandini, S., Rosso, R., 1996. Diffusion wave modelling of distributed catchment dynamics. Journal of Hydrologic Engineering – ASCE 1 (3), 103–113.

Orlandini, S., Perotti, A., Sfondrini, G., Bianchi, A., 1999. On the storm flow response of upland Alpine catchments. Hydrological Processes 13, 549–562.

Ponce, V.M., 1986. Diffusion wave modelling of catchment dynamics. Journal of Hydraulic Engineering – ASCE 112 (8), 716–727.

Ponce, V.M., Yevjevich, V., 1978. Muskingum-Cunge method with variables parameters. Journal of the Hydraulics Division – ASCE 104 (12), 1663–1667.

Ponce, V.M., Theurer, F.D., 1982. Accuracy criteria in diffusion routing. Journal of the Hydraulics Division – ASCE 108 (6), 747–757.

Refsgaard, J.C., Storm, B., 1995. MIKE SHE. In: Singh, V.P. (Ed.), Computer Models of Watershed Hydrology. Water Resource Publications, Highlands Ranch, CO.

Soil Conservation Service, 1972. National Engineering Handbook, Section 4, Hydrology. U.S. Department of Agriculture, Washington D.C.

Strahler, A.N., 1964. Quantitative geomorphology of drainage basins and channel networks, section 4-II. In: Chow, V.T. (Ed.), Handbook of Applied Hydrology. McGraw-Hill, New York.

Tarboton, D.G., 1997. A new method for the determination of flow directions and upslope areas in grid digital elevation models. Water Resources Research 33 (2), 309–319, doi:10.1029/96WR03137.

Uhlenbrook, S., Frey, M., Leibundgut, C., Maloszewski, P., 2002. Hydrograph separations in a mesoscale mountainous basin at event and seasonal time scales. Water Resources Research 38 (6), 1–14.

Uhlenbrook, S., Sieber, A., 2005. On the value of experimental data to reduce the prediction uncertainty of a process-oriented catchment model. Environmental Modelling & Software 20 (1), 19–32.

Young, D.F., Carleton, J.N., 2006. Implementation of a probabilistic curve number method in the PRZM runoff model. Environmental Modelling & Software 21 (8), 1172–1179.

Zhan, X., Huang, M.L., 2004. ArcCN-runoff: an ArcGIS tool for generating curve number and runoff maps. Environmental Modelling & Software 19 (10), 875–879.